Simulation Study of a Gramicidin/Lipid Bilayer System in Excess Water and Lipid. II. Rates and Mechanisms of Water Transport

See-Wing Chiu,*# Shankar Subramaniam,*#§¶‖ and Eric Jakobsson*#§¶‖

*National Center for Supercomputing Applications, #Department of Molecular and Integrative Physiology, §Department of Biochemistry, ¶Center for Biophysics and Computational Biology, and ‖Beckman Center for Advanced Science and Technology, University of Illinois, Urbana, Illinois 61801 USA

ABSTRACT A gramicidin channel in a fluid phase DMPC bilayer with excess lipid and water has been simulated. By use of the formal correspondence between diffusion and random walk, a permeability for water through the channel was calculated, and was found to agree closely with the experimental results of Rosenberg and Finkelstein (Rosenberg, P. A., and A. Finkelstein. 1978. *J. Gen. Physiol.* 72:327–340; 341–350) for permeation of water through gramicidin in a phospholipid membrane. By using fluctuation analysis, components of resistance to permeation were computed for movement through the channel interior, for the transition step at the channel mouth where the water molecule solvation environment changes, and for the process of diffusion up to the channel mouth. The majority of the resistance to permeation appears to occur in the transition step at the channel mouth. A significant amount is also due to structurally based free energy barriers within the channel. Only small amounts are due to local friction within the channel or to diffusive resistance for approaching the channel mouth.

INTRODUCTION

We have introduced the relevant background to molecular dynamics simulations of gramicidin channels in a companion paper on the structure of the gramicidin/lipid molecular complex (Chiu et al., 1999). The gramicidin channel has long been used as a model for permeation studies as well as structural studies. Based on the geometry of the beta-helix, one expects there to be a long single-file region of water molecules or water plus ions. This expectation was confirmed by measurements of the interaction betweem osmotic gradients and electrostatic gradients in ion transport, which revealed that the translocation of an ion involves the simultaneous translocation of 7 to 9 water molecules (Rosenberg and Finkelstein, 1978a; Levitt, 1984). Molecular dynamics studies of the solvated channel revealed long-range persistent structure and strongly coordinated water motions in the channel (Chiu et al., 1989). Because of the coordination of the individual water molecules in the chain, fluctuation analysis of the center-of-mass of the chain of water molecules in the channel, as if they constituted a single particle, provided insights about the mechanisms of translocation (Chiu et al., 1991, 1992, 1993). In the earlier molecular dynamics studies of the channel, limitations on computational power did not permit the explicit inclusion of the surrounding lipid membrane in these studies. Therefore it was necessary to impose artificial restraints on the channel protein to preserve its secondary structure. Studies were done of how the mobility and permeability of the channel contents varied with the severity of the artificial restraints. It was discovered that immobilizing the channel while maintaining the thermal motion of the lumenal contents at a normal level effectively reduced the permeability to zero (Chiu et al., 1991). (This result was later found to pertain also to a model of the sodium channel that did not have the extensive mandatory single-filing region of the gramicidin channel (Singh et al., 1996).) If the channel was less severely restrained, it was found that the mobility of water in the gramicidin channel was a sensitive function of degree of severity of restraints applied to the side chains that protrude into the lipid, even if no explicit restraints were applied to the backbone that forms the lining of the channel lumen (Chiu et al., 1992).

These results clearly suggest that the surrounding lipid has the potential to modulate the permeability of the channel, so that it would be of interest to explore the dynamics of the channel permeation in a simulated lipid environment. It has long been known that the properties of the boundary lipids surrounding a membrane protein may strongly modulate the protein's function (Warren et al., 1975; Lee, 1998). In the present paper we consider water transport properties of the channel as it is embedded in a membrane environment of excess lipid and water. This system is appropriate for simulating experimental studies of permeation through gramicidin channels, including the water permeation that is the focus of this study (Dani and Levitt, 1981; Rosenberg and Finkelstein, 1978b; Finkelstein, 1987).

The water permeability of the channel is of interest as a model of biologically important processes. Water permeability across membranes plays a vital role in osmotic balance across all living cells and in processes including transpiration and secretion. This permeability is mediated by ubiquitous water channels (Park and Saier, 1996), whose

Received for publication 5 February 1998 and in final form 19 January 1999.

Address reprint requests to Dr. Eric Jakobsson, Dept. of Biophysics, University of Illinois, 405 North Mathews Ave., 4309 Beckman Institute, Urbana, IL 61801. Tel.: 217-244-2896; Fax: 217-244-2909; E-mail: jake@ncsa.uiuc.edu.

0006-3495/99/04/1939/12 $2.00

structural motifs are beginning to be determined (Cheng et al., 1997; Li et al., 1997), as well as by the phospholipid membrane itself (Finkelstein, 1987; Marrink and Berendsen, 1994).

METHODS

The computational methodology of this paper is the same as for the companion paper (Chiu et al., 1999), and is summarized below.

The overall strategy for computing the membrane preparation with incorporation of surface tension is similar to that presented in Chiu et al., 1995. Differences are stated below. In all other respects it can be assumed that the computations in this paper are methodologically the same as the previous paper.

True constant surface tension (as opposed to constant lateral pressure) was used. The surface tension for the bilayer was set at 46 dyn/cm, based on the work of MacDonald and Simon (1987).

Following our previous published computation (Chiu et al., 1995) with a hydration level of 23 waters/lipid molecule, we computed a DMPC bilayer with 100 phospholipid molecules and 32 waters/lipid molecule and 46 dyn/cm surface tension (Chiu et al., 1996). The surface area per lipid molecule equilibrated to 61 $Å^2$ per phospholipid molecule. At the end of a 770-ps simulation we removed two phospholipid molecules from each monolayer near the center of the simulated patch and inserted a gramicidin A channel containing nine water molecules in its lumen. The coordinates for the channel were kindly supplied Drs. Roger Koeppe and Tim Cross, as determined by NMR in their labs (Ketchem et al., 1993, 1997; Koeppe et al., 1994). Our dimer was assembled with one monomer in the configuration as determined by the Cross lab and the other in the configuration as determined by the Koeppe lab.

The complete computed system consisted of a GA channel, 96 DMPC molecules, and 3209 water molecules. It was energy-minimized and then thermalized at 305 K with velocity reassignments for every 0.2 ps (100 time steps) for 50 ps. At this stage, position restraints to all GA atoms were applied with a harmonic force constant of 5000 kJ mol^{-1} $Å^{-2}$. In a subsequent MD run of 100 ps the restraining force was reduced to zero in 20 incremental step reductions of 250 kJ mol^{-1} $Å^{-2}$, with the reductions done at 5-ps intervals. The system was again thermalized at 305 K with velocity reassignments for 10 ps, and then subjected to continuous MD simulations. After 200 ps of continuous MD the system potential energy leveled off. Data collection began at this point. The data were saved at 50 fs (25 time step) intervals.

RESULTS

It is of interest to compare water permeation in the simulated gramicidin channel embedded in lipid with water permeation in our previously simulated gramicidin channel with artificial stabilizing restraints on the channel (Chiu et al., 1991, 1992). Fig. 1 shows the time course of water dipole moment projections in the channel during the 1.4-ns simulation. There is a strong tendency for the water dipoles all to be aligned in the same direction. During the run there was one transition event in which all the dipoles flipped from one orientation to the other. The event lasted 0.08 ns, from $t = 0.25$ ns, when the first water dipole flipped, until $t = 0.33$ ns, when the last water dipole flipped. Fig. 2 shows the time course of the position in the normal to the membrane plane of all the waters in the system that spent any time in the channel during the simulation. Note that the motion of the waters in the channel is in single-file register. When waters are in the channel they are significantly less mobile than when they are outside the channel. During the course of the simulation several waters enter and leave the ends of the channel. At all times there are either eight or nine waters in the channel. At any time, the column of eight or nine waters acts as a "shaking stack" (Schumaker, 1992). Specific transitions occur when a new water appends itself to a column of 8, making a column of 9, or when a water leaves one end of a column of nine, making a column of eight. From Fig. 2 it is seen that 13 waters in the system spent at least some time in the channel during the course of the simulation. Of these, six (numbers 5–10) remained in the channel throughout the entire duration of the simulation. Two, (numbers 1 and 13) began the run in bulk solution and entered the channel. Three (numbers 3, 11, and 12), began the run in the channel and left the channel to go completely into the bulk. Two (numbers 2 and 4) entered and exited the channel mouth but never made a complete transition into the

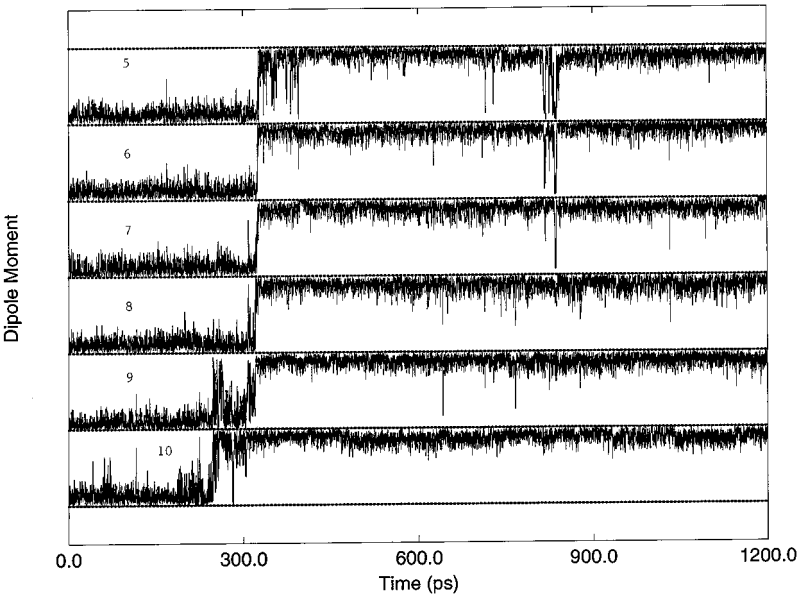

FIGURE 1 The time course of water dipole moment projections along the channel axis for the six water molecules that spent all their time in the channel. For each water molecule the dotted lines above and below the trajectory represent the water dipole moment completely aligned along the channel axis. It is seen that there is a strong tendency for the water dipole moments to be aligned in the same direction along the channel axis. It is seen that, during the course of the simulation, there is one clear transition between waters oriented in one direction and in the other direction along the channel axis.

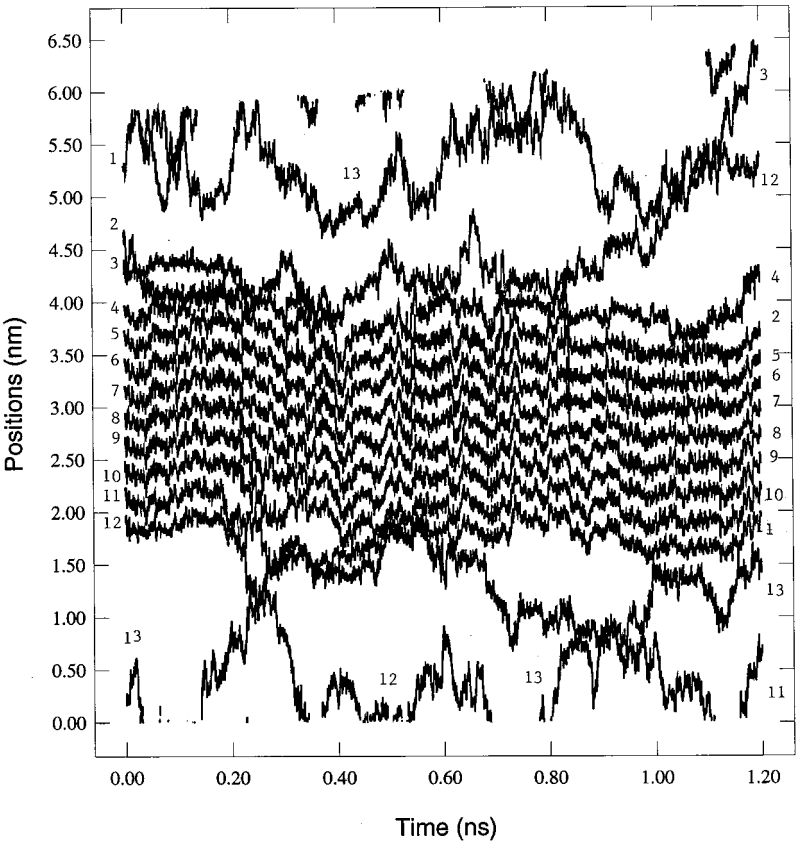

FIGURE 2 The trajectories of position along the channel axis of all the waters in the system that spent any time in the channel during the simulation. Vertical axis is position in the dimension normal to the membrane, horizontal axis is time. It is seen that the waters in the channel move in an obligatory single-file fashion and are less mobile (as seen by smaller positional fluctuations) than water outside the channel.

bulk phase. When they left the channel they remained in a region in which they interacted with phospholipid headgroups around the channel mouth.

A significant measure of the mobility of the water in the channel is the mean square deviation correlation function of the position along the channel axis of the center of mass of the chain of waters in the channel. The slope of this function is twice the diffusion coefficient of water in the channel. Fig. 3 shows this function for the calculations presented in this paper, over a short time lag (up to 10 ps). This function was calculated using the trajectories of six water molecules (numbers 5–10 in Fig. 2) that remained in the channel during the entire 1.2 ns of the computation. The MSD is shown for the individual water molecules and also for the center of mass of the chain of the six water molecules that remained in the channel throughout the duration of the

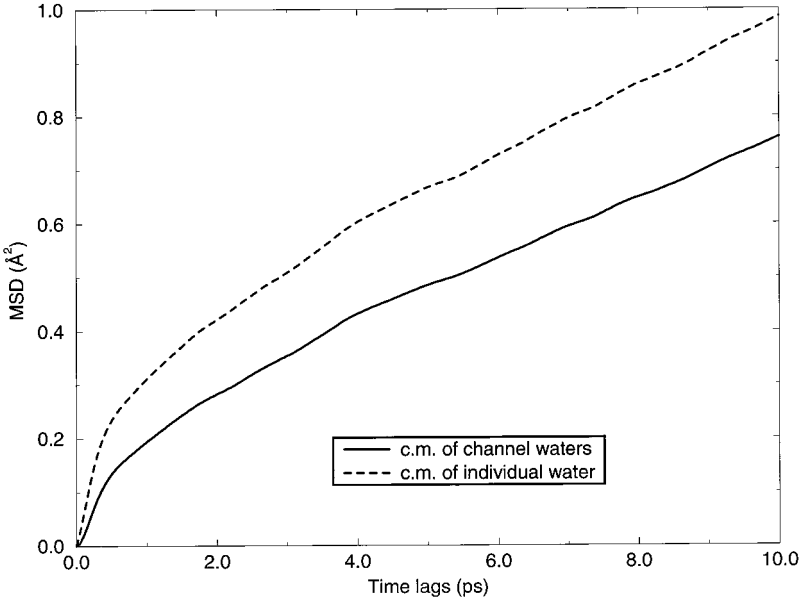

FIGURE 3 Analysis of water motions in the channel by fluctuation analysis. Plots show the mean-square-deviation correlation function versus the time-lag, for motion of the center-of-mass of the chain of six waters that were always in the channel during the run, and for motion of the individual waters that were always in the channel during the run, in the direction normal to the membrane plane. The slope of the MSD curve is just 2 times the diffusion coefficient. As a corollary, the inverse of the slope is just ½ of the diffusive resistivity. The initial slope near the origin of the curve for the individual waters defines the fluid dynamic diffusion coefficient, or local friction, for the water molecules to move within local energy wells defined by hydrogen-bonding networks to the channel and to each other. The final slope defines the effective diffusion coefficient for the chain of waters to traverse the energy barriers defined by the channel structure.

simulation (numbers 5–10). Because of the obligatory single-file nature of the water motion through the channel, the center of mass of the lumenal contents of the channel is the entity whose motion governs translocation of water through the channel (Chiu et al., 1993).

The initial slope of the MSD curve for individual molecules in Fig. 3 is determined by the local friction resisting the water motion. This slope in Fig. 3 is 0.59 $Å^2$/ps. This slope suggests that the local friction for water to move in the channel environment is close to that of bulk water, since if this slope were translated into a diffusion coefficient, it would be 3×10^{-5} cm^2/s. This is very close to the 2.7×10^{-5} cm^2/s for the self-diffusion coefficient of bulk water at this temperature. [The SPC/E water model bulk self-diffusion coefficient is in very close agreement with experiment near 300 K (Berendsen et al., 1987) and for the full temperature range from 300 to 325 K (Chiu, unpublished results)]. Thus the local friction in the channel is of a similar magnitude to that governing the diffusion of water in bulk. The final slope of Fig. 3 is proportional to the rate for the chain of waters to cross the energy barriers associated with the channel structure. The effective diffusion coefficient for water in the channel, computed from the final slope of Fig. 3, is 2.7×10^{-6} cm^2/s, or a factor of 10 lower than the self diffusion coefficient for bulk water.

Fig. 4 shows the profile of diffusion coefficients for water as a function of depth in the membrane. To get this profile, water molecules were sampled in slices 1 Å thick along the dimension normal to the membrane plane. The results were computed according to the MSD coefficient with a time lag of 4 ps for two preparations: the gramicidin/water/lipid preparation that is the subject of this paper and a pure lipid preparation (DMPC) under the same conditions as described in the Methods section of the companion paper (Chiu et al., 1999). For both preparations, the water mobility falls continually as one moves from the bathing solution to the interior of the membrane, declining overall by about one order of magnitude. Bulk water mobility is shown for comparison. It is seen that the water at the outer surface of our preparation has a mobility slightly less than bulk, indicating that we are not quite at an excess water situation. Presumably, if we had a thicker boundary of water at the surface, we would achieve bulk mobility in that boundary layer. For the pure lipid preparation there are no data from the hydrocarbon center of the membrane, because the water did not permeate that far. For the preparation containing gramicidin, it is seen that the mobility does not change dramatically at the depth corresponding to the mouth of the channel. (Note that the analysis of Fig. 4 does not distinguish between water just outside the channel mouth and water at a depth corresponding to the channel mouth but some distance from the channel in the membrane plane.) The mobility seems slightly higher in the center of the channel. This may be due to the increased flexibility in the center of the channel where the two monomers are joined, as indicated by a larger rms deviation of the backbone torsion angles in that region than elsewhere in the channel interior (Chiu et al., 1999).

Another measure of mobility is the rotational autocorrelation function of the dipole moments of the individual water molecules, $\langle \mathbf{D}(t + \tau) \cdot \mathbf{D}(t) \rangle / \mathbf{D}^2$, where $\mathbf{D}$ is the dipole moment vector of the individual water molecules. The rotational autocorrelation function as a function of depth in the membrane is shown in Fig. 5 *A* for the pure lipid membrane and in 5 *B* for the membrane containing gramicidin. It is seen that by this measure the same things are true for the water mobility as were shown in Fig. 4 by the measure of the MSD; i.e., the mobility in the boundary is a bit lower than in bulk water, the mobility decreases with depth into the membrane, and the mobility in the part of the

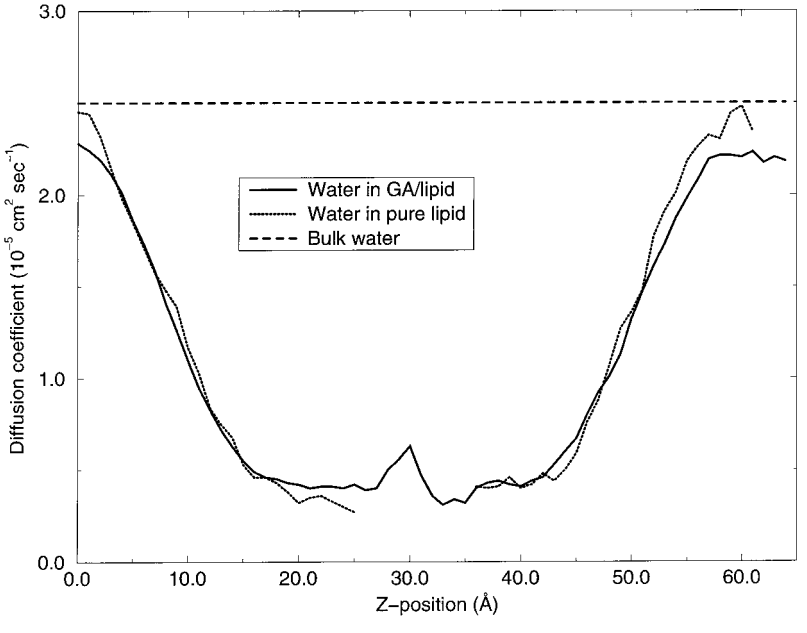

FIGURE 4 Diffusion coefficient for water as a function of depth in the membrane; i.e., position along the dimension normal to the membrane surface. The mobility profile is shown for both a pure DMPC preparation and for the DMPC/lipid preparation computed under the same conditions and the same degree of hydration. The diffusion coefficient is measured by the MSD correlation function with a time lag of 4 ps. It is seen that the water at the outer boundary is not quite as mobile as bulk water. The mobility profiles are similar in the two preparations, except that there are no waters in the deep hydrocarbon interior of the pure DMPC preparation. For the preparation containing gramicidin, the mobility does not change dramatically at the transition between the channel mouth and lipid interfacial region.

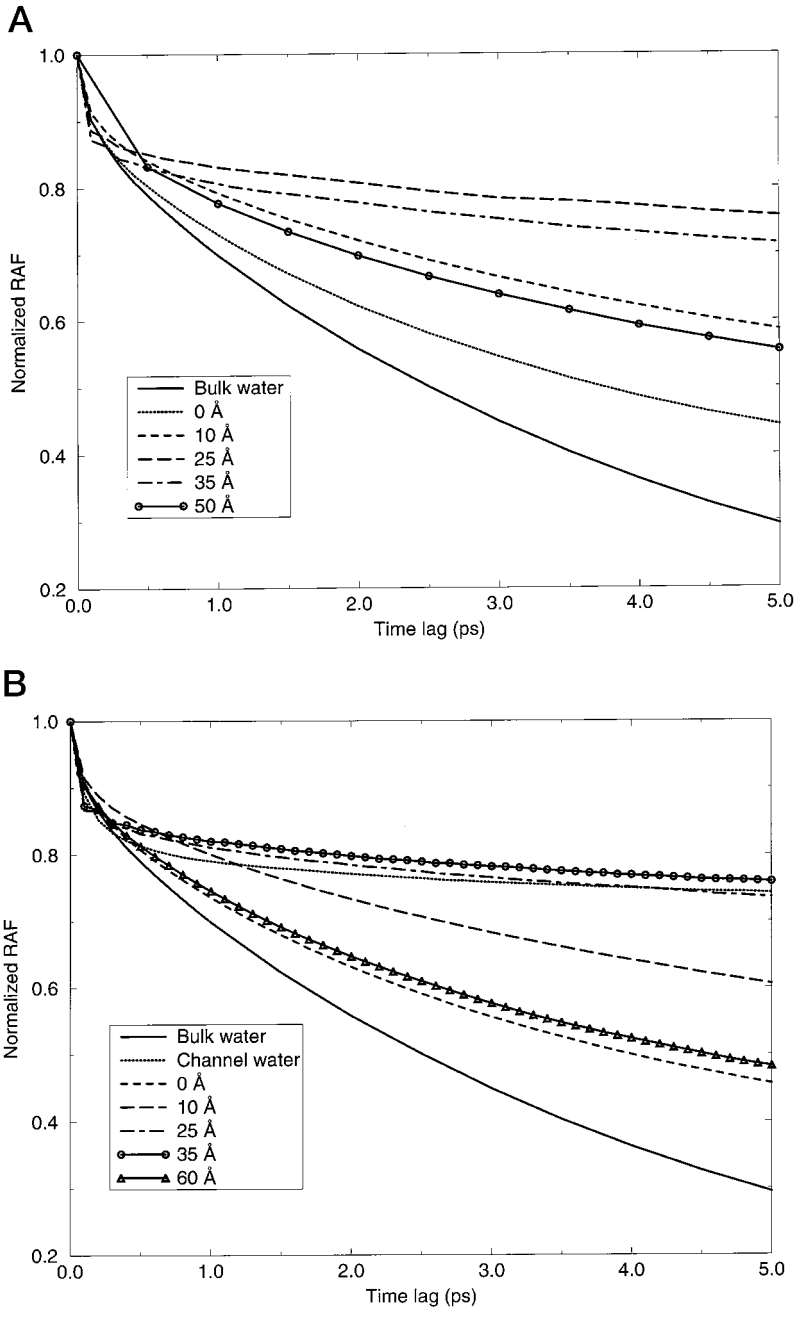

FIGURE 5 Another measure of mobility of water as function of depth in the membrane, the rotational autocorrelation function (RAF) of the dipole moments of the individual water molecules. As with the MSD, it is seen that by the RAF the water at the outer boundaries is a bit less mobile than bulk water, the mobility decreases with increasing depth into the interfacial region, and the mobility in the deepest part of the interfacial region is similar to the mobility in the channel. (*A*) Pure DMPC membrane; (*B*) membrane with gramicidin channel inserted.

interfacial region closest to the hydrocarbon is similar to that in the channel.

It is of interest to compare the diffusion coefficient in the channel with those obtained in our previous simulations of water motion in the gramicidin channel with artificial restraints on the protein. The comparison cannot be made directly because in our earlier simulations a different water model (SPC rather than SPC/E) was used. The SPC model has a higher self-diffusion coefficient in bulk than does SPC/E, by a factor of 1.8 (Berendsen et al., 1987). A reasonable method of comparison of the different computations is to see how much slower the water in the channel is than bulk water. This comparison, between the water mobility in the channel with explicit lipid around it as compared with the mobility in the channel with various artificial restraints, is shown in Table 1. The general result is that, allowing for the different mobility of the SPC relative to the SPC/E water, it seems that the simulations with relatively loose artificial restraints mimicked the effects of the lipid membrane on water mobility quite well. Two of the simulations with relatively tight restraints (0.1 ps all-atom and 4 ps side chains, 40 ps backbone) gave markedly lower water mobility.

Net water permeability in the simulation is deduced from the number of events in which water made the transition between bulk and channel. From Fig. 2 we see that there are five such events in the simulation. Let us consider each of these events as a step in a random walk. The frequency of

TABLE 1 Mobility for protein structure barrier crossing, water in the gramicidin channel

Degree of Restraint	Water Model	Absolute Mobility, cm^2/s	Relative Mobility Compared to Bulk Water
60 ps, all-atom*	SPC	6×10^{-6}	0.13
40 ps, all-atom*	SPC	6×10^{-6}	0.13
20 ps, all-atom*	SPC	6×10^{-6}	0.13
0.1 ps, all-atom (rigid channel)*	SPC	5×10^{-7}	0.01
40-ps backbone, 4-ps side chains#	SPC/E	3.5×10^{-7}	0.013
40 ps all-atom#	SPC/E	2.1×10^{-6}	0.08
40 ps backbone, unrestrained side chains#	SPC/E	3×10^{-6}	0.12
No artificial restraints, channel in explicit lipid§	SPC/E	2.7×10^{-6}	0.1

*Analyzed from Chiu et al., 1991.
#Analyzed from Chiu et al., 1992.
§Analyzed from data presented in this paper.

these events is five events in 1.2 ns, or $4.2 \times 10^9\ s^{-1}$. Since there are only five discrete events going into the calculation of the simulated effective diffusion coefficient, the statistical uncertainty in the frequency is considerable. Using the rule that the standard deviation of n events is $n^{1/2}$, we can say that the expected number of events in 1.2 ns is 5 ± 2.2, giving a frequency of $4.2 \pm 1.8\ s^{-1}$. To calculate the size of the random walk, consider that the mean water-water spacing in the channel is 2.6 Å. To effect a mean shift of the water column by 2.6 Å it is necessary for one water molecule to enter one end of the channel and another to leave the other end. Thus a singular entering or leaving event will be associated with a mean shift of 1.3 Å, or 1.3×10^{-8} cm. (We see from Fig. 2 that such singular events do occur and are associated with a fluctuation in the number of waters single-filing in the channel, usually between 8 and 9.) To compute an effective diffusion coefficient from these events, we utilize the correspondence between diffusion and random walk in one dimension noted by Einstein (1926),

$$D = nl^2/2$$

where n is the frequency of the random walk steps and l is the size. Thus the diffusion coefficient associated with these events is $(4.2 \pm 1.8 \times 10^9 \times 1.3^2 \times 10^{-16})/2\ cm^2/s = 3.5 \pm 1.6 \times 10^{-7}\ cm^2/s$. Rosenberg and Finkelstein (1978b) have measured the water permeability of gramicidin channels in a phospholipid (phosphatidylethanolamine) membrane. The value is ⅙ that of the permeability measured by Dani and Levitt (1981) in the glycerol monolein membrane, leading to a value of $2.8 \times 10^{-7}\ cm^2/s$ for the effective diffusion coefficient for the column of water in this system. It is seen that, to within the expected statistical error of the simulation, the Rosenberg-Finkelstein experiment and the simulation are in agreement.

We consider how to understand the factors determining the channel permeability. One approach is to introduce the concept of diffusive resistance. The diffusive resistance is inversely proportional to a diffusion coefficient or a permeability in just the way that an electrical resistance is inversely proportional to a conductance. The general relationship between the diffusive resistance and the effective diffusion coefficient for diffusion through a channel of length d is $R_d = d/D$. In this case d is the length of the gramicidin channel, 2.5×10^{-7} cm. Formally we can identify four types of resistance to water movement: 1) local friction that governs the magnitude of the smallest positional fluctuations of the water molecules; 2) the effects of free energy barriers associated with the specific structure of the channel peptide, with a spacing of one L-D pair of amino acids (Chiu et al., 1993); 3) the free energy barriers for water molecules to cross the channel mouth to enter and leave the channel; and 4) the diffusive resistance for a water molecule to approach the channel mouth from bulk solution. We can say that the overall resistance to permeation is the sum of the resistances from these four components. To calculate the components of the resistance, consider the following three diffusion coefficients associated with the system: D_f, the diffusion coefficient associated with local friction, D_b, the effective diffusion coefficient for barrier crossing in the channel, and D_t, the overall effective diffusion coefficient associated with the permeation of water between the bulk phases through the channel. The overall diffusive resistance of the simulated system is

$$R_{d,t} = d/D_t = 2.5 \times 10^{-7}\ cm/3.5 \times 10^{-7}\ cm^2/s = 0.7\ s/cm.$$

Let us designate the diffusive resistance associated with local friction as $R_{d,f}$, the additional diffusive resistance from the barriers in the channel as $R_{d,b}$, and the additional diffusive resistance from the "access resistance" for water molecules to exchange between the channel mouth and bulk water as R_{da}. Now we can write

$$R_{d,f} = d/D_f = 2.5 \times 10^{-7}\ cm/3 \times 10^{-5}\ cm^2/s = 0.008\ s/cm$$

$$R_{d,b} = d/D_b - R_{d,f} = 2.5 \times 10^{-7}\ cm/2.7 \times 10^{-6}\ cm^2/s - R_{d,f} = (0.093–0.008)\ s/cm = 0.085\ s/cm$$

$$R_{d,a} = R_{d,t} - R_{d,b} - R_{d,f} = (0.7 - 0.085 - 0.008)\ s/cm = 0.61\ s/cm.$$

By percentages, we can say that the local friction within the channel contributes (0.008/0.7) or 1% of the overall resistance to permeation, the structurally based free energy barriers within the channel contribute (0.085/0.7) or 12% of the overall resistance to permeation, and the resistance to waters moving between the interior of the channel mouth and bulk contributes the remainder, or 87% of the overall resistance.

The next step in the analysis is to separate the access resistance into two components: 1) diffusion up to the mouth of the channel, and 2) the free energy barrier associated with individual water molecules effecting a transition between the interior and exterior of the channel. To calculate the diffusive resistance up to the channel mouth, we cast the problem as one of radial diffusion in a nonhomogenous medium up to the channel capture radius. (The medium is nonhomogenous because of the phospholipid headgroups. Thus when we write the diffusion equation in spherical coordinates, the mobility and water concentration will be a function of r, the distance from the channel mouth, and ϕ, the angle of elevation of the position from the membrane plane.) The equation for the diffusive resistance up to the channel mouth at each end of the channel is

$$R_{\text{access}} = \int_{r=\infty}^{r=r_c} \frac{dr}{2\pi r^2 [D \cdot \exp(-\psi)]_{\text{avg}}(r)} \tag{1}$$

Where r_c is the capture radius, D is the diffusion coefficient, ψ is the dimensionless free energy (units of kT), and $[\,]_{\text{avg}}$ denotes an averaging over all values of elevation angle ϕ at a given r.

Since the diffusing species, water, is not undergoing a net driving force, its concentration can serve as a measure of the free energy via the Boltzmann relationship; i.e., $\exp(-\psi) = C^*$, where C^* is the water concentration normalized to bulk, C/C_{bulk}.

Thus the equation for the access diffusive resistance goes to

$$R_{\text{access}} = \int_{r=\infty}^{r=r_c} \frac{dr}{2\pi r^2 [D \cdot C^*]_{\text{avg}}(r)}. \tag{2}$$

Note that the expression for access resistance above is in units of time/distance^3, whereas all resistances calculated numerically in the paper up to this point are in units of time/distance. The discrepancy is because up to this point we have treated the movement through the channel as one-dimensional motion, whereas the access is treated as diffusion in a three-dimensional space. In order to make the two descriptions comparable, it is necessary to normalize by an assumed cross-sectional area of the channel. It is reasonable to postulate that the cross-sectional area is equal to πr_c^2, so that we finally arrive at an expression for the resistance to permeation due to the diffusive resistance up to the mouth of the channel is

$$R_{\text{d,ad}} = \pi r_c^2 \int_{r=\infty}^{r=r_c} \frac{dr}{2\pi r^2 [D \cdot C^*]_{\text{avg}}(r)}. \tag{3}$$

In order to calculate the access diffusive resistance from Eq. 3, it is necessary to evaluate D and C^* as a function of position in the hemispherical spaces outside the channel mouths and to postulate a reasonable value for the capture radius. Since most of the diffusive resistance for diffusion up to a sphere is very close to the sphere's surface, the outer limit of the integration on the right-hand side of Eq. 3 is taken to be $r = 18$ Å. Fig. 6, *A* and *B* show the mean water diffusion coefficient (as evaluated by the MSD correlation) and mean water normalized concentration as a function of the radial distance from a point in the center of the channel directly at the mouth out to 18 Å away. For the purposes of this calculation the channel mouth is defined as a point on the longitudinal axis of the channel and at a longitudinal position equidistant from the three outermost carbonyl oxygens lining the lumen; i.e., the carbonyl oxygens from leucines 10, 12, and 14. The logic of this definition is that the typical hydrogen-bonding pattern of water in the channel is for the carbonyl oxygens to be hydrogen-bonded to the water hydrogens (Chiu et al., 1989).The outermost water in the chain of channel waters is typically in position to be hydrogen-bonded to one of these three carbonyl oxygens. It can be seen in Fig. 6, *A* and *B* that the water becomes less mobile and less concentrated closer to the channel mouth, until the density rises at very short distances, where there is a contribution from the outermost water in the chain of waters in the channel. The "capture radius" is the radial distance at which one makes the transition from waters in the channel to waters outside the channel. Strictly speaking, this is not well-defined, because the position of the last water in the chain of channel waters is continually fluctuating, and because individual water molecules periodically either join the chain of waters from the outside or leave the chain of waters. But a reasonable criterion for the capture radius is where the water concentration starts to rise with decreasing radius, suggesting that one is entering the relatively high-density region within the channel. (The mean difference in position along the channel axis (z-position) of adjacent waters is ~2.6 Å, showing that the water density in the channel is quite high.) From inspection of Fig. 6 *A* a reasonable value for the capture radius is in the range of 1–2 Å. For comparison, it was early postulated that the capture radius is the difference between the channel radius (~2 Å) and the radius of a water molecule (~1.4 Å), or 0.6 Å (Andersen, cited in Läuger, 1976). Läuger (1976) suggested that the "effective" capture radius would be somewhat larger than 0.6 Å, and our simulations appear to bear this out. Because we are looking in a radial direction, even at large r much of the averaging is done in the headgroup region, so that even at large r the concentration and mobility do not approach the bulk values.

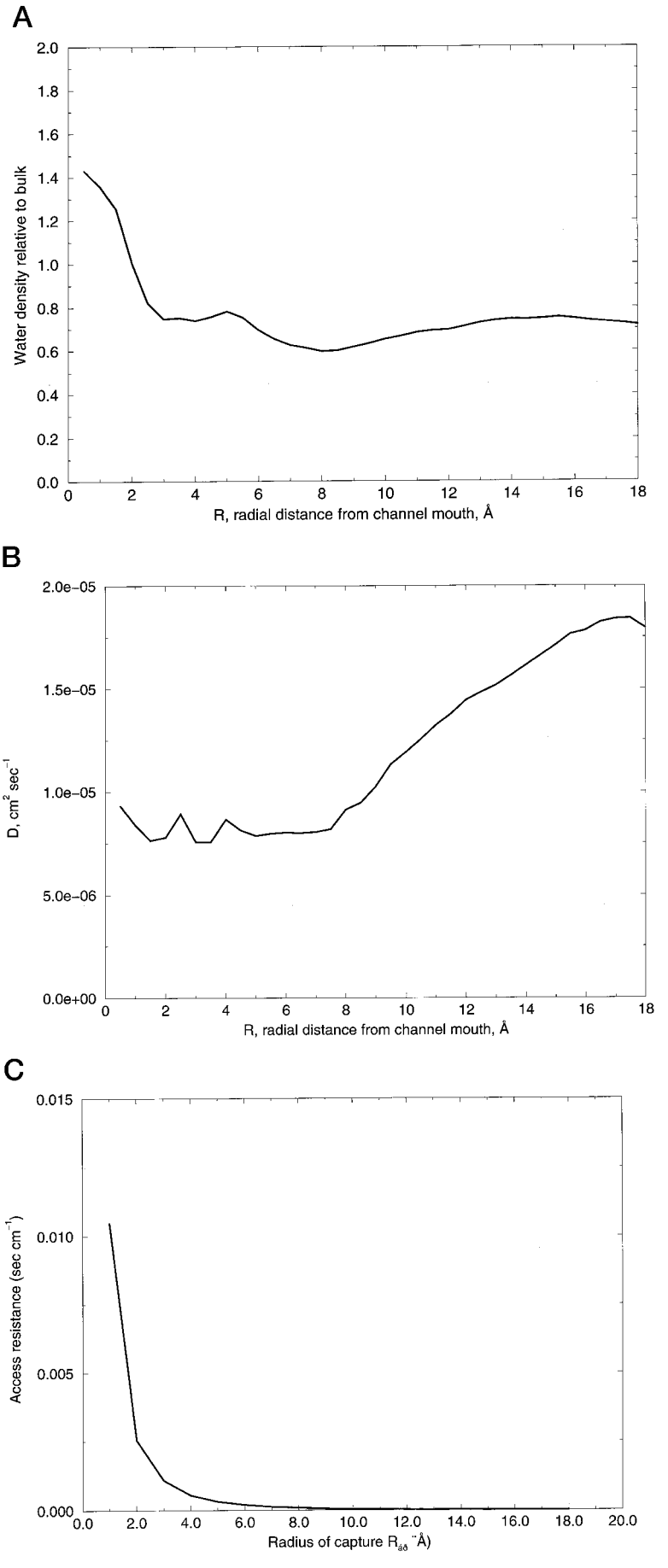

FIGURE 6 The diffusive component of the access resistance for water to diffuse up to the channel mouth. (*A*) Mean concentration of water near the channel mouth as a function of radial distance from the channel mouth center; (*B*) mean diffusion coefficient of water as a function of radial distance from the channel mouth center; (*C*) access resistance as a function of the postulated capture radius, calculated from inserting the data of (*A*) and (*B*) into Eq. 3.

Fig. 6 *C* shows the diffusive access resistance up to the capture radius using Eq. 3 and the data from Fig. 6, *A* and *B*. It is seen that for any assumed value of the capture radius that is reasonable in the light of Fig. 6 *A* (~1–2 Å) the diffusive access resistance is very small (order of 10^{-2} s/cm) in comparison to the total resistance to permeation for the region from bulk to the interior of the channel mouth. Therefore it appears that the major component of the access resistance is not diffusive, but rather is based on the discrete step of water at the channel mouth exchanging its solvation environment from that within the channel to that pertaining outside the channel.

DISCUSSION AND SUMMARY

As in previous studies without explicit lipid, we found water dipoles in the channel generally aligned with each other. However, there was a period of ~80 ps, (from ~250 to ~330 ps in Fig. 1) when the water dipoles were not lined up with each other. During this time they were making a transition from alignment in one direction to alignment in the other.

As in previous studies, we found that the water molecules in the channel moved in an obligatorily single-file manner. Thus it is reasonable to apply fluctuation analysis to the center of mass of the waters that remain in the channel during the duration of the simulation, in order to find the water permeability of the channel. In doing this analysis we obtained the following results:

The mobility for translocating across the internal structural barriers of the channel was 2.7×10^{-6} cm^2/s, or 0.1 times the bulk self-diffusion coefficient. [The SPC/E water model used in this study has almost exactly the same self-diffusion coefficient as the experimental value for bulk water (Berendsen et al., 1987). Hence the comparisons we make in this paper between water mobilities in this simulated system and water mobilities in bulk apply equally well to simulated and experimental values for bulk water.] In Table 1, the mobility for translocating the barriers within the channel is compared with the same quantity computed in previous studies in our lab with no explicit lipid, but with artificial restraints on the channel to maintain the overall structural motif. It is seen that the mobility with explicit lipid around the channel is comparable to that with relatively light artificial restraints. Note in Table 1 that the mobility of the channel lumen contents are quite sensitive to restraints on the side chains, even though the side chains do not line the lumen of the channel. From these comparisons we infer that the lipid environment of the gramicidin channel does not exert a significant restraint on the protein motions necessary to facilitate water transport across the channel.

The local diffusion coefficient for moving within the channel structural barriers was 3×10^{-5} cm^2/s, or 1.1 times the bulk self-diffusion coefficient. Thus the local diffusion coefficient for the water in the channel is not very different from the self-diffusion coefficient for bulk water. By some usages, this local diffusion coefficient as we define it would not be termed a diffusion coefficient at all, since it does not quantify the rate-limiting process for translocation of the water through the channel. We use it here as the quantity that is inversely proportional to the local friction according to the Einstein relationship, $D = kT/(m\zeta)$, where ζ is the local friction coefficient for motions within the local potential well defined by water-water spacing in the channel (Chiu et al., 1993). Our description in this paper of the barrier-crossing motions for water in the channel are very similar to those in our earlier paper, in which the membrane was emulated with artificial restraints (Chiu et al., 1993). They are in some contrast to a view from Roux and Karplus (1991) of water motion in the channel as essentially free diffusion. In general the orientations and motions described by Roux and Karplus for the gramicidin system are similar to ours. We ascribe the difference with respect to this particular point to a different type of analysis, in which they analyzed the motions of individual water molecules, while our analysis is of the center-of-mass of the chain of waters in the channel. The reasoning behind our analysis that, since the water motion is obligatorily single-file, the functional unit for transfer across the membrane is the chain of waters.

By considering the diffusional resistances for the system to be inversely proportional to the permeabilities, we can calculate the contribution of each of the three resistive components of the system to the overall diffusional resistance. The total diffusive resistance is just the reciprocal of the overall permeability, or 0.7 s/cm. The contribution of the

TABLE 2 Comparison between water mobilities based on analysis of simulation data in this paper and experimental water mobilities

Computed Result Based on Analysis of Simulations Reported in This Paper	Experimental Result Most Closely Related to Computed Result
Fluid dynamic diffusion coefficient of water in the gramicidin channel, 3×10^{-5} cm^2/s	Self-diffusion coefficient of water in bulk, 2.7×10^{-5} cm^2/s*
Effective diffusion coefficient for water to translocate free energy barriers within channel, 2.7×10^{-6} cm^2/s	Effective diffusion coefficient for water to permeate gramicidin in membrane without bulky headgroups, 1.7×10^{-6} cm^2/s#
Effective diffusion coefficient for water to translocate across channel between bulk water phases, 3.5×10^{-7} cm^2/s	Effective diffusion coefficient for water to permeate gramicidin in membrane with bulky headgroups, 2.8×10^{-7} cm^2/s§

*Mills, 1973.
#Dani and Levitt, 1981.
§Rosenberg and Finkelstein, 1978.

local friction is 0.008 s/cm, or 1%. The contribution of the gramicidin structural barriers is 0.085 s/cm, or 12%. The contribution of the "access resistance," the entering and exiting of the waters at the channel mouth past the restricted area bounded by the phospholipid headgroups, is 0.61 s/cm, or 87%. These three components of diffusional resistance can be interpreted as three different values of the diffusion coefficient for water in the system, as shown in Table 2.

From the analysis around the data presented in Fig. 6, we found that the diffusive component of the access resistance is quite small. Practically all of the access resistance, and indeed the majority of the resistance to permeation for water across the channel from one bulk phase to the other, comes from the rate at which water can transform its hydration environment from that of the channel interior to that of the exterior, at the channel mouth.

The large contribution of the step at the channel mouth to the overall resistance to permeation of the channel suggests a reason for the discrepancy between the two published experimental values for the single channel water permeability of gramicidin. The experiment that gave the larger value (Dani and Levitt, 1981) was done in a glycerol monolein membrane that lacked headgroups. The experiment that gave the smaller value, by a factor of 6 (Rosenberg and Finkelstein, 1978b), was done in a phosphatidylethanolamine membrane, in which one might expect headgroups to impinge on the access of water molecules to the channel mouth, as shown in Fig. 7. This figure shows a snapshot (instantaneous configuration) of the channel by itself (*image on the left*) and the channel plus the membrane (*image on the right*) looking down normal to the membrane plane. The water has been removed from the visualization. In the left image note the channel opening in the center of the structure. In the right image, note that phospholipid headgroups have impinged on the area over the channel mouth, suggesting that the solvation environment just outside the channel mouth is significantly modified by the headgroups.

The results presented in this paper point up the necessity of including the total environment of the channel in a model system if one is to adequately characterize the permeation process in a simulation.

Our overall single channel permeability estimates should be considered quite approximate, since even a 1.2-ns simulation is not long enough to gather very good statistics on water molecules entering and leaving the channel. From inspection of Fig. 2, there appeared to be just five distinct

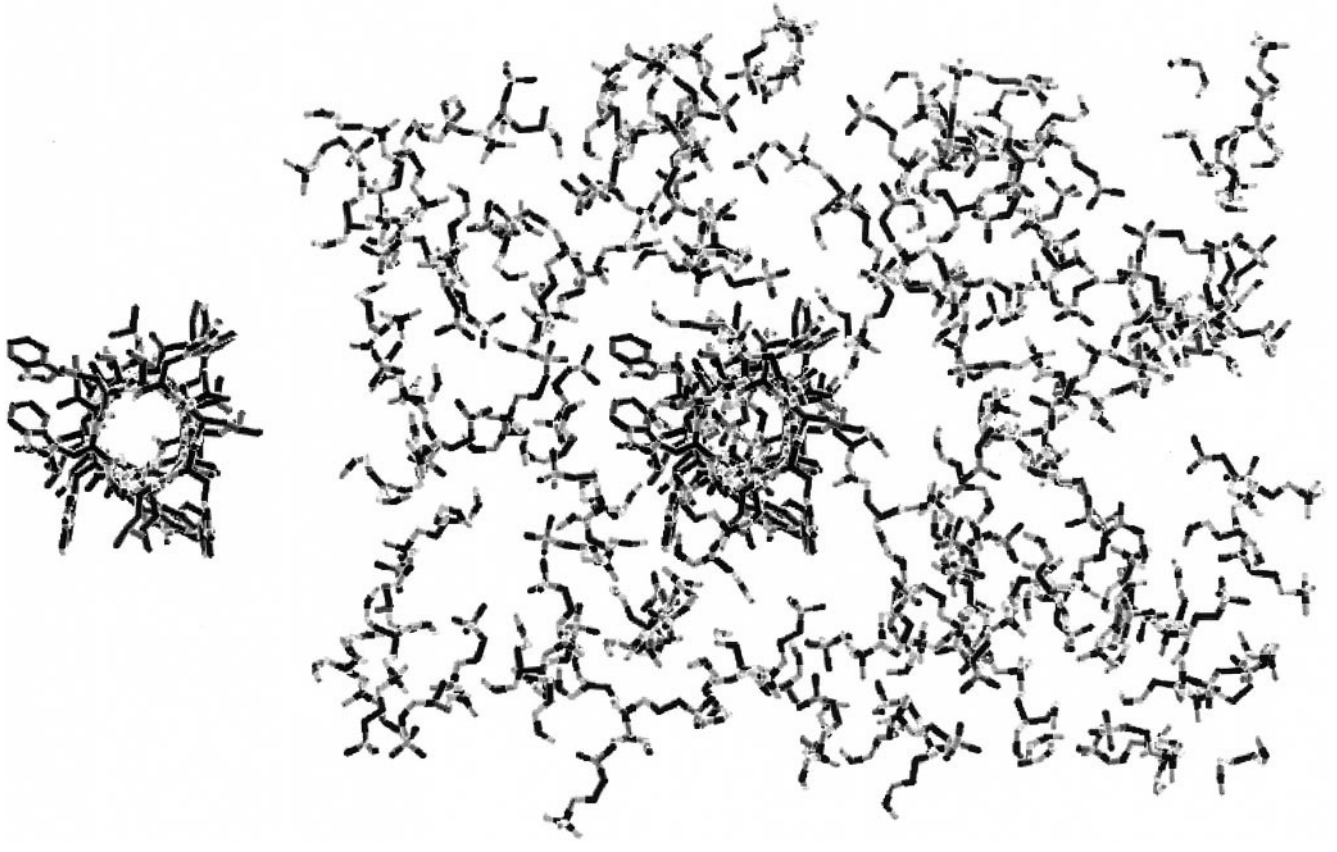

FIGURE 7 Snapshot view of the gramicidin channel and the membrane lipid headgroups, viewed from above the surface in a bond structure representation. (*A*) Gramicidin channel alone, clearly showing the pore through the center of the channel. Note the clearly visible pore through the center of the channel. (*B*) Channel plus the lipid headgroups. It is seen that the headgroups in the lipids adjacent to the channel impinge into the region around the mouth of the channel. The crowding of the phospholipid headgroups around the mouth of the channel is a possible structural basis for modification of the solvation environment around the mouth of the channel.

events in which a water molecule either joined the chain of water molecules in the channel after being clearly in the bulk phase (numbers 1 and 13 in Fig. 5 *B*) or left the chain of waters to move completely into the bulk phase (numbers 3, 11, and 12 in Fig. 5 *B*). This is such a small number that its interpretation as proportional to a macroscopic rate, as we have done in this paper, is certainly subject to large statistical error. However, we can say with certainty that the overall permeation rate is much lower than it would be if there were no significant resistance beyond that of the channel lumen itself. We can extrapolate the diffusion rate for internal barrier crossing, 2.7×10^{-6} cm^2/s, to the number of expected events for water to enter or leave the channel in the 1.2-ns simulation if there were no significant access resistance. This is done by the relationship

$$n = 2Dt/l^2$$

where l is the shift in the position of the water column position for each such event, ~1.3 Å. This calculation results in an expectation of 32 water molecules leaving or joining the column of water in the channel during the simulation. The difference between 5, the observed number, and 32, the number expected in the absence of access resistance, is clearly highly significant. Therefore we can say with confidence that the access resistance is a large fraction of the overall diffusive resistance of the system. The imprecision of the computed value for the access resistance arises solely because the access resistance is so large; if it were smaller, we would have been able to compute it more precisely.

The above analysis extracts diffusive behavior from our MD results via fluctuation analysis, and shows how the net effect of the diffusion can be analyzed as a small number of effectively discrete transitions in the mean position and composition of the column of waters in the channel. As such this analysis forms a bridge between continuum diffusive and "hopping" descriptions of permeation in channels (see Hille, 1992, especially Ch. 10). The specific picture of the fluctuating movement of the column of waters with waters leaving or joining the ends of the column bears a strong formal resemblance to the "shaking stack" model for permeation in a narrow channel proposed by Schumaker (1992). The analysis also shows that major components of permeation may not be amenable to a description in terms of diffusion. The hydration transition at the channel mouth between extralumenal and lumenal hydration environments is too localized to be described by diffusion theory; it is essentially a discrete event. Thus we have found that the full description of water permeation across the gramicidin channel involves a combination of diffusive and discrete processes.

Hladky (1987) has suggested that the access resistance for ion permeation of gramicidin is dominated by a hydration/dehydration step at the channel mouth, as we have found to be the case for water. This may also be the case for describing permeation through potassium channels as well, since the high-resolution structure of the potassium channel permeation pathway (Doyle et al., 1998) shows two regions that are narrow enough to imply single-filing of water and ions, necessitating distinct hydration/dehydration transitions at four points in the permeation pathway.

We should note that our results do not necessarily imply that the access resistance dominates in the same way for ion permeation of gramicidin as it apparently does for water permeation in phospholipid membranes. In both experiment and simulation, the mobility of the channel lumen contents for translocation within the channel is much lower when an ion is present in the channel than when only water is in the channel (Chiu et al., 1993). Indeed, the measurement of water permeability through gramicidin channels depends on this fact. Water permeability is measured by the reduction in water flux with increased permeant ion concentration, based on the assumption that water permeation through a gramicidin channel is almost completely blocked by ion occupancy (Rosenberg and Finkelstein, 1978b; Dani and Levitt, 1981). Thus the channel component of the overall resistance to permeation may be relatively significantly higher for ions than for water.

Much analysis of experimental results has assumed that the behavior of the gramicidin channel is essentially the same in glycerol membranes and in phospholipid membranes. This is certainly a reasonable assumption for many types of behavior. Our results suggest that with respect to the specific phenomenon of water permeation, the observed experimental difference in channel permeability between the channel in glycerol and phospholipid membranes is real rather than artifactual, and is due to a different hydration environment for water just outside the channel mouth in the two environments. Given the particular interactions between aromatic side chains and the interfacial region in phospholipid membranes, the shape of the lipid surface in the vicinity of the channel may be different in the two types of membranes. In general, possible effects of the lipid environment should be considered when analyzing experimental results from these two types of membrane environments.

The authors are grateful to Roger Koeppe and Tim Cross for providing NMR-derived coordinate files for the initial configurations of the gramicidin monomers.

This work was supported by a grant from the National Science Foundation. Computations were done on the Silicon Graphics Power Challenge Array at the National Center for Supercomputing Applications.

REFERENCES

Berendsen, H. J. C., J. R. Grigera, and T. P. Straatsma. 1987. The missing term in effective pair potentials. *J. Chem. Phys.* 91:6289–6291.

Cheng, A., A. N. van Hoek, M. Yeager, A. S. Verkman, and A. K. Mitra. 1997. Three-dimensional organization of a human water channel. *Nature*. 387:627–630.

Chiu, S.-W., M. Clark, V. Balaji, S. Subramaniam, H. L. Scott, and E. Jakobsson. 1995. Incorporation of surface tension into molecular dynamics simulation of an interface: a fluid phase lipid bilayer membrane. *Biophys. J.* 69:1230–1245.

Chiu, S.-W., K. Gulukota, and E. Jakobsson. 1992. Computational approaches to understanding the ion channel-lipid system. *In* Membrane Proteins: Structures, Interactions, and Models. A. Pullman, B. Pullman, and J. Jortner, editors. Kluwer, The Netherlands.

Chiu, S.-W., E. Jakobsson, S. Subramaniam, and J. A. McCammon. 1991. Time-correlation analysis of simulated water motion in flexible and rigid gramicidin channels. *Biophys. J.* 60:273–285.

Chiu, S.-W., J. A. Novotny, and E. Jakobsson. 1993. The nature of ion and water barrier crossing in a simulated ion channel. *Biophys. J.* 64:98–108.

Chiu, S.-W., S. Subramaniam, and E. Jakobsson. 1996. Simulation of a fully hydrated DMPC bilayer using the NγT boundary conditions. *Biophys. J.* 70:94*A*. (Abstr.).

Chiu, S.-W., S. Subramaniam, and E. Jakobsson. 1999. Simulation study of a gramicidin/lipid bilayer system in excess water and lipid. I. Structure of the molecular complex. *Biophys. J.* 76:000–000.

Chiu, S.-W., S. Subramaniam, E. Jakobsson, and J. A. McCammon. 1989. Water and polypeptide conformations in gramicidin channels: a molecular dynamics study. *Biophys. J.* 56:253–261.

Dani, J. A., and D. G. Levitt. 1981. Water transport and ion-water interactions in the gramicidin channel. *Biophys. J.* 35:501–508.

Doyle, D. A., J. M. Cabral, R. A. Pfuetzner, A. Kuo, J. M. Gulbis, S. L. Cohen, B. T. Chait, and R. MacKinnon. 1998. The structure of the potassium channel: molecular basis of K+ conduction and selectivity. *Science*. 280:69–77.

Einstein, A. 1926. Investigations on the Theory of the Brownian Movement. Translation by A. D. Cowper of papers published 1905–1908. R. Furth, editor. Dover Publications, New York.

Finkelstein, A. 1987. Water Movement through Lipid Bilayers, Pores, and Plasma Membranes. Theory and Reality. Wiley-Interscience, New York.

Hille, B. 1992. Ionic Channels of Excitable Membranes. Sinauer, Sunderland, MA.

Hladky, S. B. 1987. Models for ion transport in gramicidin channels: how many sites? *In* Ion Transport Through Membranes. K. Yagi and B. Pullman, editors. Academic Press, Tokyo. 213–232.

Ketchem, R. R., W. Hu, and T. A. Cross. 1993. High-resolution conformation of gramicidin A in a lipid bilayer by solid-state NMR. *Science*. 261:1457–1460.

Ketchem, R. R., B. Roux, and T. A. Cross. 1997. High-resolution polypeptide structure in a lamellar phase lipid environment from solid state NMR derived orientational constraints. *Structure*. 5:1655–1669.

Koeppe, R. E. II, J. A. Killian, and D. V. Greathouse. 1994. Orientations of the tryptophan 9 and 11 side chains of the gramicidin channel based on deuterium nuclear magnetic resonance spectroscopy. *Biophys. J.* 66:14–24.

Lee, A. G. 1998. How lipids interact with an intrinsic membrane protein: the case of the calcium pump. *In* In Search of a new Biomembrane Model O. G. Mouritsen and O. S. Andersen, editors. Munksgaard, Copenhagen. 115–120.

Levitt, D. 1984. Kinetics of movement in narrow channels. *Curr. Top. Membr. Transp.* 21:181–198.

Li, H., S. Lee, and B. K. Jap. 1997. Molecular design of aquaporin-1 water channel as revealed by electron crystallography. *Nat. Struct. Biol.* 4:263–265.

MacDonald, R. C., and S. A. Simon. 1987. Lipid monolayer states and their relation to bilayers. *Proc. Natl. Acad. Sci. USA*. 84:4089–4093.

Marrink, S. J., and H. J. C. Berendsen. 1994. Simulation of water transport through a lipid membrane. *J. Phys. Chem.* 98:4155–4168.

Mills, R. 1973. Self-diffusion in normal and heavy water in the range 1–45 degrees. *J. Phys. Chem.* 77:685–688.

Park, J. H., and M. H. Saier, Jr. 1996. Phylogenetic characterization of the MIP family of transmembrane channel proteins. *J. Membr. Biol.* 153:171–180.

Rosenberg, P. A., and A. Finkelstein. 1978a. Interactions of ions and water in gramicidin A channels. Streaming potentials across lipid bilayer membranes. *J. Gen. Physiol.* 72:327–340.

Rosenberg, P. A., and A. Finkelstein. 1978b. Water permeability of gramidicin A-treated lipid bilayer membranes. *J. Gen. Physiol.* 72:341–350.

Roux, B., and M. Karplus. 1991. Ion transport in a gramicidin-like channel: dynamics and mobility. *Biophys. J.* 95:4856–4868.

Schumaker, M. F. 1992. Shaking stack model of ion conduction through the Ca^{2+}-activated K^+ channel. *Biophys. J.* 63:1032–1044.

Singh, C., S. Sankararamakrishnan, S. Subramaniam, and E. Jakobsson. 1996. Solvation, water permeation, and ionic selectivity of a putative model for the pore region of the voltage-gated sodium channel. *Biophys. J.* 71:2276–2288.

Warren, G. B., M. D. Houslay, J. C. Metcalfe, and N. J. M. Birdsall. 1975. Cholesterol is excluded from the phospholipid annulus surrounding an active calcium transport protein. *Nature*. 255:684–687.